Prenatal inhibition of the tryptophan - kynurenine pathway alters synaptic plasticity and protein expression in the rat hippocampus

Caroline M Forrest[1*], Omari S. Khalil[1*], Mazura Pisar[1], L Gail Darlington[2], Trevor W Stone[1]

[1] Institute for Neuroscience and Psychology, University of Glasgow, West Medical Building,

Glasgow G12 8QQ, U.K.

and

[2] Epsom General Hospital, Dorking Road, Epsom, Surrey, UK, KT18 7EG

Running title: - Kynurenines and brain development

Correspondence: - Prof. T. W. Stone, West Medical Building, University of Glasgow, Glasgow, UK G12 8QQ.

Key-words:- kynurenines; kynurenic acid; tryptophan; neurodevelopment; Rho proteins; sonic hedgehog; doublecortin

* CMF and OSK contributed equally to this work

Abstract

Glutamate receptors sensitive to N-methyl-D-aspartate (NMDA) are important in early brain development, influencing cell proliferation and migration, neuritogenesis, axon guidance and synapse formation. The kynurenine pathway of tryptophan metabolism includes an agonist (quinolinic acid) and an antagonist (kynurenic acid) at these receptors. Rats were treated in late gestation with 3,4-dimethoxy-N-[4-(3-nitrophenyl)thiazol-2-yl]-benzene-sulphonamide (Ro61-8048), an inhibitor of kynurenine-3-monoxygenase which diverts kynurenine metabolism to kynurenic acid. Within 5h of drug administration there was a significant decrease in GluN2A expression and increased GluN2B in the embryo brains, with changes in sonic hedgehog at 24h. When injected dams were allowed to litter normally, the brains of offspring were removed at postnatal day 21 (P21). Recordings of hippocampal field excitatory synaptic potentials (fEPSPs) showed that prenatal exposure to Ro61-8048 increased neuronal excitability and paired-pulse facilitation. Long-term potentiation was also increased, with no change in long-term depression. At this time, levels of GluN2A, GluN2B and postsynaptic density protein PSD-95 were all increased. Among several neurodevelopmental proteins, the expression of sonic hedgehog was increased, but DISC1 and dependence receptors were unaffected, while raised levels of doublecortin and Proliferating Cell Nuclear Antigen (PCNA) suggested increased neurogenesis. The results reveal that inhibiting the kynurenine pathway *in utero* leads to molecular and functional synaptic changes in the embryos and offspring, indicating that the pathway is active during gestation and plays a significant role in the normal early development of the embryonic and neonatal nervous system.

1. Introduction

Receptors for glutamate, especially NMDA receptors, are intimately involved in the early formation of the central nervous system (CNS), being required for neuronal migration (Komuro and Rakic, 1993; Behar et al., 1999), axonal and neurite growth in the foetus and postnatally, neurite extension and branching (Heng et al. 1999; Cuppini et al. 1999; Rajan and Cline 1998), spine formation and stability (Alvarez et al., 2007; Ultanir et al., 2007), the formation and stability of synapses (Colonnese et al., 2005) and neuronal plasticity (Fagiolini et al,. 2003; Iwasato et al., 2000). In rodents, NMDA receptor blockade during late foetal or early postnatal life also provokes a substantial loss or disruption of synapses compared with control animals (Dikranian et al., 2001; Ikonomidou et al., 1999; Harris et al., 2003), partly mediated by the p53 tumour suppressor gene whose expression is controlled by NMDA receptors (Poulakie et al., 1999). The neuronal loss produces profound abnormalities of neuronal development, brain structure and behaviour reminiscent of those seen in schizophrenia (Harris et al., 2003; du Bois and Huang, 2007). In humans, a similar neuron loss occurs from the sixth month *in utero* until the third year of life, making it potentially susceptible to external modification and thus a potential source of pathology and of therapeutic intervention.

The use of extraneous compounds activating or blocking NMDA receptors, however, does not provide any indication of whether there is any natural, physiological system which normally regulates activity of these receptors by modulating the levels of endogenous agonists, antagonists or transduction systems. Such a pathway could modify the activation of NMDA receptors in response to external agents or events. One endogenous pathway which is known to include compounds capable of modifying NMDA receptor function is the kynurenine pathway of tryptophan oxidative metabolism (Stone, 1993, 2001; Stone and Darlington, 2002). This pathway - the major route of tryptophan metabolism - includes quinolinic acid, an agonist at NMDARs (Stone and Perkins, 1981) and kynurenic acid

which is an antagonist at all ionotropic glutamate receptors, though with greatest potency at NMDARs (Perkins and Stone, 1982) and with some ability to block nicotinic receptors in the CNS (Hilmas et al., 2001; Stone, 2007). The ratio between the levels of quinolinic acid and kynurenic acid is known to influence overall neuronal excitability (Scharfman et al., 1999) and survival after CNS interventions (Boegman et al., 1985; Clark et al., 2005; Rodgers et al., 2010) when their levels are altered acutely in adult animals. This ratio can be modified by inhibiting kynurenine-3-monoxygenase (KMO)(Cozzi et al., 1999; Chiarugi et al., 2001; Chiarugi and Moroni, 1999; Clark et al., 2005; Zwilling et al., 2012).

Since the kynurenine pathway is potentially able to modulate NMDA receptor function and those receptors are important in neural development, this study was designed to address the question of whether the normal, physiological activity of the kynurenine pathway plays any role in brain development. The pathway has been inhibited using the KMO inhibitor 3,4-dimethoxy-N-[4-(3-nitrophenyl)thiazol-2-yl]-benzene-sulphonamide (Ro61-8048) (Rover et al., 1997), which has been administered to gestating female rats and the effects have been examined on the expression of proteins in the CNS of the embryos and neonates. The target molecules examined play key roles in neuronal development, neurite outgrowth, synapse formation and neurotransmitter release. They include components of synaptic vesicle and neurotransmitter release machinery and structural proteins associated with formation of the cytoskeleton. Several markers of axon guidance and synapse formation are included, as well as Nuclear Factor kappa B (NFkB) and cyclo-oxygenase 2 (COX-2). Since metabolites of the kynurenine pathway modulate the activity of NMDA receptors, the proteins examined include the NMDA receptor subunits, and the Postsynaptic Density Protein-95 (PSD-95). Finally, the neuronal maturation molecule doublecortin and the cell proliferation indicator Proliferating Cell Nuclear Antigen (PCNA) were included.

Protein expression was examined in embryos 5 and 24 hours after the administration of Ro61-8048 and in the brains of offspring at 21 days of age (P21), the time of weaning. The data reveal immediate effects of kynurenine pathway inhibition on NMDA receptor expression with additional, substantial changes at P21 in the expression of several proteins of importance to brain development. An electrophysiological examination of neuronal excitability and plasticity in the hippocampus indicates there are also significant functional differences between drug-treated and control animals. The results imply that the kynurenine pathway is of fundamental importance in early brain development.

2. Results

2.1 HPLC analysis of kynurenines

The ability of Ro61-8048 to inhibit KMO in pregnant animals was confirmed using HPLC. Levels of kynurenic acid were increased 100-fold in the maternal plasma after 5h and from undetectable concentrations to 13pmols/g wet weight in the maternal brain (Fig. 1B). Comparable, substantial, increases were seen in the brains of the embryos. After 24h, kynurenine and kynurenic acid concentrations had decreased to basal levels in the maternal brain, although they remained significantly elevated in the embryonic brains (Fig. 1B).

At P21, there were no differences in the levels of tryptophan, kynurenine or kynurenic acid between pups born to dams treated with Ro61-8048 and those receiving vehicle (data not shown). Thus, the neurochemical and electrophysiological changes observed at P21 are likely to be the result of interference with brain development around the time of the injections *in utero*, rather than any long-term effects of Ro61-8048 on tryptophan metabolism persisting at P21.

2.2 Effects of prenatal Ro61-8048 on embryonic brains during gestation

In the embryo brains, 5h and 24h after maternal administration of Ro61-8048, the expression was examined of the NMDA receptor subunits GluN1, GluN2A and GluN2B, as well as COX-2, NFkB, PCNA, SHH, Sox-2, EphA4, actin and PSD-95. There were no significant changes in the levels of most of these proteins or in the expression of the ubiquitous GluN1 subunit of NMDA receptors. However substantial, significant, changes were induced by 5h in both of the NMDA receptor subunits GluN2A and GluN2B, with a 43% reduction of GluN2A and a 395% increase in the level of GluN2B (Fig. 2A). There were also significant increases in expression of the morphogenetic protein sonic hedgehog and NFkB after 24h (Fig. 2B).

2.3 Effects of prenatal Ro61-8048 in P21 neonates

2.3.1 Hippocampal function

Field excitatory postsynaptic potentials (fEPSPs) in the stratum radiatum and population spikes in stratum pyramidale were evoked to assess neuronal excitability and synaptic transmission (Fig. 3). Stimulus strength was increased until the fEPSP began to show signs of a population spike. The slices from animals treated with Ro61-8048 were more excitable than slices from control animals (ANOVA, $F = 53.19$, $P < 0.0001$, $n = 16$ controls, 15 treated) with 3 individual points significantly different (Bonferroni test for multiple comparisons) (Fig. 3A). A similar result was obtained using population spike amplitude, with a significant increase in Ro61-8048-exposed slices at corresponding current intensities (ANOVA, $F = 73.84$, $P < 0.0001$, $n = 12$), with 3 individual points significantly different (Fig. 3B).

Paired-pulse facilitation (PPF) and paired-pulse inhibition (PPI) were examined using stimulus pairs with interpulse intervals from 100ms to 10ms. There was a tendency for greater PPF in slices from drug-exposed animals (ANOVA, $F = 4.4$, $P = 0.0004$, $n = 10$

controls, 12 treated) (Fig. 3C) but there were no significant differences between individual points (Bonferroni test). A similar trend was apparent using population spikes (ANOVA, $F = 10.81$, $P < 0.0001$) but with no significant differences between individual points (Fig. 3D). The effect of the rate at which stimulus pairs are presented was also examined as the rate was increased from 0.1Hz to 1Hz (Fig. 3E). No differences were seen between treated and control slices at presentation rates of 0.1, 0.2, or 0.5Hz, but at 0.5Hz or greater paired-pulse effects in control slices changed from PPF to PPI (Fig. 3E). In contrast PPF was observed at all presentation rates in Ro61-8048-exposed slices, leading to significant differences between the slices (ANOVA, $F = 21.32$, $P < 0.0001$, with significant differences at 0.5 ($P < 0.01$) and 1Hz ($P < 0.001$) presentation.

Long-term potentiation (LTP) was induced using a burst of theta stimulation (5 bursts per second, for 2 seconds, of 4 stimuli delivered at 100Hz) (Larson et al. 1986). In control slices this increased fEPSP amplitude which reached a plateau after approximately 20min and was stable until the end of the recording period (Fig. 4A-C). A comparison of fEPSP size over the 5min before stimulation and the final 5min after theta stimulation showed a significant difference (ANOVA, $F = 8.76$; $P < 0.0001$, $n = 5$) with an increase of 28.2% between mean fEPSP slopes before and after LTP induction ($P < 0.0001$, paired t test, $n = 5$).

For slices prepared from animals exposed to Ro61-8048 administration *in utero*, LTP was obtained with a similar time course but a higher magnitude than in control slices (Fig. 4A). The fEPSP slopes were significantly greater than the corresponding pre-stimulation level (ANOVA, $F = 41.25$; $P < 0.0001$, $n = 5$) with an increase of 46.4% between the mean fEPSP slope before and after theta stimulation ($P = 0.002$, paired t test, $n = 5$). This LTP was significantly larger in treated animals compared with controls (ANOVA, $F = 9.10$, $P < 0.0001$, $n = 5$), with significant differences ($P < 0.01$) for each of the final 5 time points (Fig. 4A).

Long-term depression (LTD) was induced using our published protocol (Forrest et al. 2011) of trains of 3 pulses at 200Hz delivered every second for 5mins (stim1, Fig. 4D-F), repeated 20mins later (stim2). In slices from control animals, LTD was obtained in which the fEPSP slope between 25-30min after stim2 was very significantly lower than in the 5min baseline period preceding stim1 (ANOVA, $F = 4.60$, $P = 0.0003$, $n = 5$), with a reduction of 19.8% between the fEPSP immediately preceding stim1 and at the end of recording ($P < 0.0001$, $n = 5$) (Fig. 4D). Slices from animals exposed to Ro61-8048 showed a similar degree of LTD ($F = 6.84$, $P < 0.0001$, $n = 5$) with a reduction of fEPSP slope by 24.7% between the potentials before and after stimulation ($P < 0.0001$, $n = 5$) (Fig. 4D). The level of LTD produced in control and drug-exposed slices was not significantly different over the final 5 minutes ($F = 0.20$, $P = 0.99$).

2.3.2. Protein expression

In addition to the expression of proteins studied for the acute response to Ro61-8048 in embryos, the levels were examined of the synaptic vesicle release proteins synaptophysin, synaptotagmin and Vesicle Associated Membrane Protein-1 (VAMP-1; synaptobrevin), the small molecular weight GTPases RhoA and RhoB, the axonal guidance and contact determinants Unc5H1, Unc5H3, EphA4 and Deleted in Colorectal Cancer (DCC), tyrosine hydroxylase (TH), α-synuclein, Disrupted in Schizophrenia-1 (DISC1), the 5HT2c receptor and proteins associated with neuronal proliferation (PCNA and doublecortin).

2.3.3. Synaptic proteins

Levels of the GluN1 subunit of the NMDA receptor were not significantly different in animals exposed *in utero* to Ro61-8048 compared with controls ($p = 0.49$, Fig. 5), but there were significant differences in expression of the GluN2 subunits. Both the GluN2A ($p = 0.004$), and the GluN2B subunits ($p = 0.03$) were increased in the test animals relative to

controls (Fig. 5). There was also a significantly increased level of the post-synaptic density protein PSD-95, which is part of the post-synaptic protein complex which includes the NMDA receptor combinations ($p = 0.03$, Fig. 5).

Of the various proteins associated with synaptic vesicle release, synaptophysin showed a trend towards increased expression ($p = 0.09$) while synaptotagmin, a putative calcium sensor for vesicular release, and synaptobrevin (Vesicle Associated Membrane Protein-1; VAMP-1) did not show any differences between control and treated animals ($p = 0.33$, $p = 0.57$ respectively).

2.3.4. Structural proteins

The two small GTPase enzymes RhoA and RhoB were examined since they have been shown to modulate or contribute to plastic changes induced electrophysiologically in the hippocampus (O'Kane et al. 2003a,b; McNair et al., 2010). Their activity is closely related to functions of NMDA receptors and they also play major roles in the regulation of cytoskeletal proteins. While there was no significant difference in the levels of RhoA between test and control pups ($p = 0.94$), there was a highly significant decrease in the expression of RhoB ($p = 0.003$, Fig. 5).

2.3.5. Developmental molecules

Since the hypothesis underlying this work was that disturbance of the kynurenine pathway *in utero* would change the expression or function of molecules responsible for early neuronal migration, axon guidance or synapse formation, the levels of several proteins with well characterised roles in these processes were examined. Levels of two major dependence receptors - the unc5H1 and unc5H3 proteins - showed no change in the Ro61-treated animals ($p = 0.52$, $p = 0.87$ respectively). Expression of the EphA4

receptor for secreted ephrin molecules was unchanged in the treated pups (p = 0.96) (data not shown).

Proliferating Cell Nuclear Antigen (PCNA), a protein often studied as a marker of the earliest phases of DNA synthesis which precede cell division and neurogenesis in the brain, was more highly expressed in the treated animals compared with controls (p = 0.02, Fig. 6). Similarly, expression of doublecortin, a molecule linked particularly with neurogenesis and the early stages of neuronal migration was significantly increased in the brains of pups exposed to Ro61-8048 (p = 0.03, Fig. 6). The sonic hedgehog protein (SHH), which is intimately involved in the polarisation and orientation of tissues and cell growth, was reduced to a significant extent after exposure to Ro61-8048 (p = 0.017, Fig. 6) while levels of the Sox-2 protein were unchanged (p = 0.45, data not shown).

2.3.6. Catecholamine-related proteins

Development of dopaminergic neurons is of particular interest in the understanding and possible prevention of the 'neurodevelopmental disorders' of schizophrenia and autism as well as neurodegenerative disorders such as Parkinson's disease. The levels were examined of several molecules with a particular relevance to the development or function of dopaminergic neurons. These included tyrosine hydroxylase (TH), the initial enzyme in the conversion of dietary tyrosine to catecholamines. The mean level of expression of TH was only 60% of that in control animals, but this difference did not reach statistical significance (p = 0.18, Fig. 6).

It has been claimed that levels of α-synuclein are increased in neurons of the nigrostriatal pathway of patients with Parkinson's disease, a disorder attributed to degeneration of the pathway. The aggregation of α-synuclein can cause neuronal degeneration and any factor which alters its expression might have a corresponding facilitatory or inhibitory effect upon susceptibility to Parkinson's disease. In this study,

Ro61-8048 did not modify the levels of α-synuclein in the P21 rat hemispheres ($p = 0.31$, Fig. 6).

Two other molecules linked with dopaminergic function are Disrupted in Schizophrenia-1 (DISC1) and the $5HT_{2C}$ receptor. Levels of the former are reduced in patients with schizophrenia while the $5HT_{2C}$ receptor is believed to exert an important modulating influence on the activity of neurons in the ventral tegmental mesolimbic pathway, and of their release of dopamine. The expression of both these proteins was unaffected after exposure to Ro61-8048 (DISC1: $p = 1.00$, Fig. 6; $5HT_{2C}$ $p = 0.22$, data not shown).

2.3.7. Inflammatory status

Finally, levels of the inflammation transcription factor Nuclear Factor kappa-B (NFkB), and the inducible form of cyclo-oxygenase (COX-2), whose expression is usually linked to inflammation-induced oxidative stress, were examined. While there was no change in the levels of COX-2 in treated animals ($p = 0.64$), there was a significant increase in the expression of NFkB ($p = 0.017$) (data not shown).

2.4 Effects of Ro61-8048 on cytokine levels

The administration of a foreign substance might induce an inflammatory response, and cytokines and chemokines can affect neuronal development. A sample of maternal blood was therefore collected into 20U/ml heparin by cardiac puncture 5h after the administration of Ro61-8048. Using Signosis ELISA profiling kits (Caltag Medsystems, Buckingham, UK) to measure cytokine levels in 6 animals showed no change in basal levels of interleukin-1β (IL-1β, $p = 0.64$), IL-1α ($p = 0.59$), IL-6 ($p = 0.93$), tumour necrosis factor-α (TNF-α; $p = 0.58$), monocyte chemoattractant protein-1 (MCP-1; $p = 0.17$), macrophage inflammatory protein-1α (MIP-1α; $p = 0.51$), Regulated on Activation, Normal T cell expressed and

secreted (RANTES) (p = 0.79) or interferon receptor (p = 0.79). These results exclude any interference by those inflammatory mediators in the changes observed here.

3. Discussion

The synthetic compound Ro61-8048 is one of the few substances known to inhibit selectively a central enzyme in the kynurenine pathway, KMO. It is well documented that Ro61-8048 generates a shift in the ratio of kynurenic acid and quinolinic acid (Chiarugi et al., 2001; Chiarugi and Moroni, 1999; Rover et al., 1997; Cozzi et al., 1999) with increased tissue kynurenate (Rover et al., 1997) and extracellular dialysate levels of 10-fold or more (Urenjak and Obrenovitch, 2000). Nevertheless, since the metabolic status of animals is substantially altered in the later stages of gestation we felt it appropriate to confirm the activity of Ro61-8048 in our model. The compound was able to generate raised kynurenine and kynurenic acid levels within a few hours of administration and we propose that these changes are responsible for the protein and functional changes we have reported. The conventional view of the kynurenine pathway would predict that inhibition of KMO would also lead to a decreased concentration of quinolinic acid, but studies have repeatedly failed to show any alteration in quinolinic acid concentrations despite substantial increases in kynurenic acid levels (Chiarugi & Moroni, 1999; Clark et al., 2005). This would suggest that quinolinic acid production can occur independently of KMO activity, possibly via an alternative, direct oxidation of anthranilic acid to 3-hydroxyanthranilic acid (Baran & Scwarcz 1990; Ueda et al.,1978). This scheme would be consistent with the dramatic increase in brain anthranilic acid concentrations we have reported in mice treated with Ro61-8048 (Clark et al., 2005). These factors emphasise our contention that the effects of Ro61-8048 reported here are more likely to be caused by increased kynurenic acid levels than to a decline in quinolinic acid production."

The 10-fold increases in kynurenine concentration produced by Ro61-8048 are generally greater than the 2-5-fold changes seen in a range of clinical conditions in humans (Chen & Guillemin 2009). However, there was no lasting effect of Ro61-8048 on the kynurenine pathway since the levels of tryptophan, kynurenine, kynurenic acid and anthranilic acid were normal by the age of P21. Thus, the molecular and functional changes we have observed at P21 are likely to be the result of interference with brain development over a relatively short period during gestation, resulting in changes in the absolute or relative amounts of developmentally relevant processes, or alterations in their rate of change during development.

It should be noted that fetal cells do express IDO so that tryptophan entering from the maternal circulation can be converted into kynurenine (Honig et al., 2004; Ligam et al. 2005). In addition, IDO expression is high in the placenta itself and the kynurenine generated from its activity will cross the placental barrier readily into the fetus.

The results show that prenatal exposure to an inhibitor of KMO produces a range of significant molecular and physiological changes in the young offspring. NMDA receptors have well-established roles in the early migration of neural precursors, neuritogenesis, axonal guidance, spine formation and synapse formation (Colonnese et al., 2005; Komuro and Rakic, 1993; Behar et al., 1999; Heng et al., 1999; Cuppini et al., 1999; Rajan and Cline, 1998; Alvarez et al., 2007; Ultanir et al., 2007). Furthermore, NMDAR contribute to the programmed cell death which shapes the early nervous system by eliminating a proportion of neurons. Many of these same factors are involved in neuronal plasticity in the postnatal brain (Fagiolini et al., 2003; Iwasato et al., 2000). Indeed, it has been proposed that tissue formation and polarity may be determined largely by a gradient for a signal antagonist, such as kynurenic acid, rather than an agonist (Gurdon and Bourillot, 2001).

Perhaps the most surprising result from this work is the magnitude and selectivity of the changes in protein expression found in the embryonic brain 5h after exposure to Ro61-

8048. None of the developmentally specific target molecules showed any change in their overall expression at this time, indicating no immediate change of guidance or contact processes and, most importantly, no direct effects of Ro61-8048 on the proteins examined. In contrast there were large, highly significant changes in the levels of the two NMDA receptor subunits GluN2A and GluN2B. In addition, the changes observed were in opposite directions, with a decreased level of GluN2A and increased GluN2B. The importance of this may lie in the requirement for a specific balance between these subunits, with a shift in their relative expression occurring progressively throughout development. The balance between these two subunits is critical in regulating neuronal function and early brain development (Brigman et al., 2010; McKay et al., 2012; Rammes et al., 2009) as well as cell viability and degeneration (Hardingham and Bading, 2010).

By the time the newborn litter has reached 21 days of age, the situation is dramatically changed. The changes of NMDA receptor composition are still exclusively in the GluN2 subunits, with no significant effects on the GluN1 subunits which contribute the crucial, universal element to all NMDAR. Although the GluN1 subunit is encoded by one gene, the protein is expressed as several splice variants. The antibody used in this work was selected as it interacts with all of the known splice variants, generating some confidence in the absence of any change in GluN1 expression. The continuing change in the expression of both GluN2 subunits, however, would produce significant overall changes in NMDAR function leading to alterations in neuronal development and function.

The electrophysiological analysis indicates an overall increase in neuronal excitability and altered synaptic function which is likely to result from a combination of altered neuronal development and the abnormal levels and ratio of GluN2 subunits. Slices from control and treated animals exhibited similar PPF across the range of interpulse intervals from 20 to 100ms. While PPI is usually attributed to the depletion of synaptic vesicles following the first stimulus (Rosenmund and Stevens, 1996; Wang and Kaczmarek,

1998), PPF is caused by the accumulation of calcium within synaptic terminals, leading to increased transmitter release and an increased size of the second potential of the pair (Zucker, 1989). The similar degrees of PPI and PPF, therefore, suggest no changes in either of these phenomena after Ro61-8048 exposure.

In contrast, changes were observed when paired-pulse interactions were examined at different frequencies of paired-pulse delivery. Increasing the frequency of stimulation from 0.05 to 1Hz has been shown previously to induce a shift from PPF to PPI in the hippocampus (Saviane et al. 2002) and a similar shift can be induced by raising stimulation strength (Huang et al. 2007). In the present study, increasing stimulation frequency converted PPF to PPI in control slices, whereas Ro61-8048-treated slices exhibited reduced PPF but no PPI, resulting in very significant differences between control and treated slices at presentation frequencies of 0.5Hz or greater.

Exposure to Ro61-8048 *in utero* led to an increase in the level of theta-burst-induced LTP with no change in the degree of LTD. The specificity of the phenomenon was emphasised by the absence of any significant difference in the amplitude of LTD. The occurrence of these various electrophysiological differences emphasise the ability of Ro61-8048 exposure *in utero* to generate significant changes in neuronal and synaptic function. The examination of protein expression was performed to identify some of the molecular changes that might contribute to this.

3.1 Protein expression

In addition to the altered expression of GluN2 subunits, several of the neurodevelopmental proteins examined also exhibited marked changes. The tyrosine kinase family of Eph receptors and their ephrin ligands are crucial to many aspects of neuronal development and synaptogenesis (Klein et al., 2004), and several of them modulate the activation of RhoGTPases. These molecules play similar and overlapping

roles, with EphA4 clearly linked to dendritic spine formation (Martinez and Soriano, 2005; Bourgin et al., 2007; Segura et al., 2007) and the formation of glutamatergic synapses (Aoto et al., 2007). The Eph receptors directly influence NMDAR function and may mediate the developmental and plastic consequences of activating NMDAR (Henderson et al., 2001; Takasu et al., 2002). However, the present data indicate no significant change in the expression of EphA4, despite the significant changes in NMDA subunits, suggesting that the altered expression of NMDAR protein is not secondary to any change of EphA4 expression.

A highly significant change was also seen in levels of RhoB. The activation of glutamate receptors and their roles in synaptic plasticity are influenced by both the low molecular weight RhoGTPases RhoA and RhoB. Li et al., (2002) were among the earliest to note an association between glutamate receptors and the activation of RhoGTPases, showing these enzymes mediated the effects of NMDA receptors on dendritic arborisation. This is probably dependent on the regulation of cytoskeletal components which determine cell polarity and motility as well as neuritogenesis (Narumiya et al., 1997; Luo, 2000). They are also likely to play a role in other neuronal responses to NMDA (Harris et al., 2003; Norenberg et al., 1999) including excitotoxicity and neuronal development (Koh et al., 2006; Ahnert-Hilger et al., 2004; van Aelst and Cline, 2004). The two enzymes have different cellular localizations in the rat hippocampus and exhibit differential changes in response to electrical stimulation (O'Kane et al., 2003a,b; McNair et al., 2010). Activation of RhoA results in the suppression of synaptic plasticity, whereas RhoB enhances the extent of neuronal plasticity in response to the activation of NMDAR. The activation of RhoB was especially promoted by high frequency stimulation which induced NMDAR-dependent LTP (O'Kane et al., 2003b). RhoA was not involved in this phenomenon. Consistent with this putative role for RhoB in NMDA receptor-dependent plasticity, inhibition of the target enzyme Rho-associated coiled coil protein kinase (ROCK) modified

the induction of LTP. The significant decrease in RhoB expression at P21, therefore, would be consistent with increased decreased amplitudes of LTP.

The inhibition of kynurenine metabolism yielded no changes in the presynaptic vesicular release proteins synaptophysin, synaptotagmin and synaptobrevin (VAMP-1). This negative result is especially interesting in view of reports that changes in the levels of synaptophysin and VAMP-1 occur in brain tissue from schizophrenic patients (Halim et al., 2003; Maycox et al., 2009; Nadri and Agam, 2009). It is possible, however, that changes may have occurred before the P21 time point at which they were first examined in this study, since Afadlal et al (2010) reported that prenatal stress induced by maternal restraint or corticosterone injections produced a decrease in synaptophysin levels only in animals at P7 or P14, but not at later ages such as the P21, post-weaning time examined here.

3.2 Neurogenesis

The nuclear protein PCNA is increasingly adopted as a marker for the early phases of cell generation in view of its function as a cofactor in the synthesis and repair of DNA (von Bohlen und Halbach, 2011). The significant increase in expression of PCNA therefore suggests a greater degree of neurogenesis in the brain at P21. This conclusion is strongly supported by the increased expression of doublecortin which has been linked to the later aspects of neurogenesis in the earliest stages of brain formation, being widely viewed as a marker of newly formed but immature or undifferentiated cells. The levels of doublecortin tend to diminish as brain development proceeds and neurogenesis decreases (von Bohlen und Halbach, 2011). The continuing presence of doublecortin in the mature CNS tends to be greatest in regions with the highest rates of neurogenesis, and its significant elevation in the experimental animals here would be consistent with a higher rate of new neuron formation and with the increased PCNA discussed above.

Also consistent with this conclusion is the significantly increased expression of SHH, a protein known to be intimately involved in early tissue development, organization and orientation. SHH is expressed largely in fully differentiated neurons (Sims, 2009) and has most frequently been studied in relation to early cell proliferation and migration (Palma et al., 2005; Traiffort et al., 2001, 2010), although it has a major role to play in the mutual attraction between growing neurites and their targets both in nervous system development and in the early phases of regeneration after tissue injury (Hor and Tang, 2010; Angot et al., 2008; Traiffort et al., 2010). The change in SHH therefore may be a key factor in the altered expression of other proteins and in the functional changes demonstrated here.

4. Materials and methods

This study was carried out according to the regulations of the Animals (Scientific Procedures) act 1986 of the UK, administered and monitored by the Home Office. Male and female Wistar rats were housed together for mating and inspected daily for the occurrence of a vaginal plug. The pregnant females were housed alone from that point, with free access to food and water.

In order to inhibit tryptophan oxidation along the kynurenine pathway (Fig. 1A) we have used 3,4-dimethoxy-N-[4-(3-nitrophenyl)thiazol-2-yl]benzenesulphonamide (Ro61-8048; Roever et al., 1997). This compound is an inhibitor of kynurenine-3-monoxygenase (KMO), a key enzyme in the pathway which shifts the balance of tryptophan metabolism such that the production of the NMDAR agonist, quinolinic acid, is reduced or the antagonist kynurenic acid is increased *in vivo* (Rover et al., 1997; Cozzi et al., 1999; Chiarugi and Moroni, 1999; Urenjak and Obrenovitch, 2000; Chiarugi et al., 2001; Clark et al., 2005; Gregoire et al., 2008) or in vitro (Carpenedo et al., 2002). From those earlier studies we

have already identified a dose of 100mg/kg (i.p.) as one which can be administered repeatedly to the same animal with few ill-effects in adult rats.

Results from two series of experiments are reported in this study. In one set, Ro61-8048 was administered to pregnant dams on embryonic day E18, partly in order to demonstrate that this dose was sufficient to produce a significant change in the levels of kynurenic acid. An additional objective was to examine the immediate effects of Ro61-8048 on the levels of kynurenine metabolites and protein expression in the embryo brains measured after 5h and 24h.

In the second series of experiments, Ro61-8048 was administered to the pregnant dams on embryonic days E14, E16 and E18, after which gestation was allowed to proceed normally. The neonates were then euthanised on postnatal day 21 (P21), the day of weaning, for removal of the brain. Dams in the control groups were injected with vehicle only, administered in the same time schedule as the test compound. All tissue samples were frozen at -80°C until analysis.

4.1 High Pressure Liquid Chromatography (HPLC)

The High Performance Liquid Chromatography (HPLC) system used for the analysis of the kynurenine pathway was modified from that used previously in this laboratory. In brief, L-kynurenine was quantified by absorbance detection spectrometry, while kynurenic acid levels were measured using fluorescence detection based on the original description by Hervé *et al.* (1996).

During sample preparation, samples were kept on ice. To 250μl plasma, 25μl of internal standard (240μM 3-nitro-L-tyrosine) and 25μl 2M perchloric acid were added. Plasma samples were vortexed for 30s immediately after acid addition, centrifuged at 5000 *g* for 10 minutes at 4°C, and the supernatant collected. Brain sample extracts were prepared by homogenising in 2 volumes (w/v) of 2M perchloric acid containing 3-nitro-L-

tyrosine internal standard (240μM). Homogenates were centrifuged at 10000 *g* for 10 minutes at 4°C and the supernatant collected. All supernatants were then filtered in MicroSpin PVDF centrifuge tubes (Alltech, Carnforth, Lancashire, UK) using centrifugation at 10,000 *g* for 10 minutes at 4°C, prior to injection of 100μl on to the HPLC column. Calibration curves were determined using various concentrations of standard compounds in solution.

Isocratic reversed-phase HPLC was performed at 37°C, using a Waters HPLC system. For tryptophan, kynurenine and kynurenic acid determination, separation was achieved using a Synergi Hydro column (250 x 4.6mm I.D., particle size 4μm; Phenomenex, Macclesfield, Cheshire, UK) and the detection system included both a Waters 2487 dual wavelength absorbance detector and a Waters 474 fluorescence detector, connected in series. The mobile phase was 50mM acetic acid, 100mM zinc acetate containing 1.5% acetonitrile using a flow rate of 1ml/min. Zinc acetate was included in the mobile phase as it significantly enhances the fluorescence of kynurenic acid (Shibata, 1988). Tryptophan was determined by absorption spectrometry at a wavelength of 250nm and kynurenine was detected at 365nm. The internal standard, 3-nitrotyrosine, was also quantified at 365nm. Fluorescence detection was used to quantify kynurenic acid (excitation 344nm, emission 390nm).

The limits of detection using an injection volume of 100μl and a signal-to-noise threshold of 3, were: tryptophan 20pmoles, kynurenine 1pmole and kynurenic acid 0.2pmoles on column. Recoveries determined using samples spiked with standards of the measured compounds were between 90 and 110%.

4.2 Electrophysiology

Electrophysiological studies were performed on male animals which were allowed to grow under normal conditions to 21 days of age (P21 animals). Animals were killed by

administration of an overdose of urethane (1.5g per rat delivered as an i.p. injection of a 25% solution in water) followed by cervical dislocation. The brain was removed into ice-cold artificial cerebrospinal fluid (aCSF) of composition: (in mM) NaCl 115; KH_2PO_4 2.2; KCl 2; $MgSO_4$ 1.2; $NaHCO_3$ 25; $CaCl_2$ 2.5; glucose 10, gassed with 5%CO_2 in oxygen. The hippocampi were rapidly removed and chopped into 450μm transverse slices using a McIlwain tissue chopper. The slices were preincubated at room temperature for at least 1 hour in a water-saturated atmosphere of 5%CO_2 in O_2 before individual slices were transferred to a 1 ml capacity superfusion chamber for recording. Slices were superfused at 28-30°C using aCSF at a flow rate of 3-4 ml/min. A concentric bipolar electrode was used for stimulation of the Schaffer collateral and commissural fibres in stratum radiatum, using stimuli delivered at 0.1 Hz or 0.05 Hz with a pulse width of 50-300 μs, adjusted to evoke a response amplitude approximately 70% of maximum so as to allow increases or decreases in size to be detected. Extracellular recordings were made via glass microelectrodes containing 1M NaCl (tip diameter approximately 2μm, DC resistances 2-5MΩ) with the tip positioned under microsopic visualisation in the stratum radiatum of the CA1 region to evoke field excitatory postsynaptic potentials (fEPSPs). Potentials were amplified, digitised and stored on computer via a CED (Cambridge Electronic Design, Cambridge, UK)) micro1401 interface. The fEPSPs were routinely quantified by measurement of the early positive-going slope of the potential, using Signal software (CED, Cambridge, UK). The axonal volley was monitored wherever it was possible to distinguish it clearly from the fEPSP in order to ensure that no change occurred during the experiments.

Once placed into the recording chamber, the recording of fEPSPs was allowed to stabilise and a minimum period of 10min obtained at a stable baseline. The degree of LTP and LTD was quantified by measuring the size of the evoked potentials once a post-

stimulation plateau had been obtained and comparing with the potential size before stimulation.

Paired-pulse interactions were assessed using pairs of stimuli S1 and S2 with inter-stimulus intervals of 10 -100ms. In the case of fEPSPs the 10ms interval resulted in a substantial overlap between successive potentials and an electronic subtraction was therefore performed (using Signal software, CED) in which a single evoked potential at time S1 was subtracted from a subsequent paired-pulse response to reveal the true magnitude of the response to S2.

4.3 Immunoblotting

Brain sample homogenates were prepared in RIPA buffer (50mM Tris, 150mM NaCl, 0.1% SDS, 0.5% Triton X-100, 1% IGEPAL, and a Roche complete protease inhibitor tablet) and centrifuged at 18000 *g* for 5 min at 4^{o}C. Supernatants were collected for protein concentration determination using the Bio-Rad Coomassie Blue protein assay (Bio-Rad, Hemel Hempstead, UK). Samples were then normalised to 10μg and prepared as; 65% protein sample, 25% sample buffer and 10% reducing agent (Life Technologies, Paisley, UK), and heated at 70^{o}C for 10 min. The protein samples were loaded onto NuPAGE Novex 4-12% Bis-Tris (1.0mm) 15 lane gels (Life Technologies, Paisley, UK) and run at 150 volts for 80 min to separate proteins according to their molecular weight. SeeBlue pre-stained standard (Life Technologies, Paisley, UK) was included on each gel as a molecular weight marker. The separated proteins were then blotted onto Invitrolon poly(vinylidene difluoride) membranes (Life Technologies, Paisley, UK) at 30V for 60 min. The membranes were blocked for 1h in 5% non-fat dried milk solution in Tris-buffered saline containing 0.05% Tween (TBST), before overnight incubation at 4^{o}C with the appropriate primary antibody (diluted in 5% milk-TBST). Membranes were then washed 3 times for 15 min with TBST and incubated with the appropriate horseradish peroxidase

(HRP) conjugated secondary antibody (prepared in 5% milk-TBST) for 1h at room temperature. Following secondary antibody incubation, blots were washed 3 times for 15 min with TBST then visualised using Enhanced Chemiluminescence Plus detection kit (GE Healthcare, Chalfont St Giles, UK).

Western blot analysis was carried out using the following primary antibodies:- PSD-95 (rabbit monoclonal, 3450, 1 : 10000 dilution) (Cell Signalling, New England Biolabs, Hitchin, UK); DCC (mouse monoclonal, 554223, 1 : 5000 dilution) (BD Biosciences, Oxford, UK); GluN1 (mouse monoclonal, 05-432, 1 : 1000 dilution postnatal tissue, 1 : 500 dilution embryonic tissue), tyrosine hydroxylase (mouse monoclonal, MAB5280, 1 : 10000 dilution), synaptophysin (mouse monoclonal, MAB368, 1 : 40000 dilution) (Millipore, Watford, UK); GluN2A (rabbit polyclonal, PPS012, 1 : 5000 dilution postnatal tissue, 1 : 1000 dilution embryonic tissue), GluN2B (rabbit polyclonal, PPS013, 1 : 5000 dilution postnatal tissue, 1 : 1000 dilution embryonic tissue), VAMP-1/synaptobrevin (goat polyclonal, AF4828, 1 : 10000 dilution), synaptotagmin (MAB 43641, 1 : 5000 dilution) (RandD Systems, Abingdon, UK); RhoA (mouse monoclonal, sc-418, 1 : 1000 dilution), RhoB (mouse monoclonal, sc-8048, 1 : 1000 dilution), EphA4 (rabbit polyclonal, sc-921, 1 : 5000 dilution), PCNA (mouse monoclonal, sc-56, 1 : 1000 dilution), Sox-2 (goat polyclonal, sc-17320, 1 : 250 dilution postnatal tissue, 1 : 1000 dilution embryonic tissue), 5-HT2C (mouse monoclonal, sc-17797, 1 : 1000 dilution), NFkB (rabbit polyclonal, sc-372, 1 : 5000 dilution postnatal tissue, 1 : 1000 embryonic tissue), COX-2 (goat polyclonal, sc-1745, 1 : 1000 dilution), doublecortin (goat polyclonal, sc-8066, 1 : 1000 dilution postnatal tissue, 1 : 20000 dilution embryonic tissue), α-synuclein (mouse monoclonal, sc-65500, 1 : 1000 dilution), actin (goat polyclonal, sc-1615, 1 : 10000 dilution postnatal tissue, 1 : 20000 dilution embryonic tissue), DISC1 (goat polyclonal, sc-47990, 1 : 1000 dilution postnatal tissue, 1 : 500 dilution embryonic tissue), Unc5H1 (goat polyclonal, sc-67902, 1 :

1000 dilution), Unc5H3 (goat polyclonal, sc-54442, 1 : 1000 dilution), SHH (goat polyclonal, sc-1194, 1 : 1000 dilution) (Santa Cruz, Insight Biotechnology, Wembley, UK).

The following secondary HRP-conjugated antibodies were used at 1 : 5000 dilution: goat anti-rabbit HRP (12-348) (Millipore, Watford, UK); donkey anti-goat HRP (sc-2020) and goat anti-mouse (sc-2005) (Santa Cruz, Insight Biotechnology, Wembley, UK)

4.4 Data analysis and statistics

All western blots were quantified using the Image J software (http://rsb.info.nih.gov/ij/) and comparisons were made statistically between groups of pups born to mothers treated with Ro61-8048 and groups born to mothers injected with saline vehicle. This protocol allowed the use of unpaired *t* tests to examine differences between the two groups for the blots, cytokine ELISAs and HPLC data. In order to control for variations in the total amount of protein loaded onto gels, all samples were examined after staining with Ponceau S stain. In addition, actin levels were examined in each series of blots and the ratio taken of the intensity of target protein to the intensity of actin. For the parts of the electrophysiological analysis where indicated, data were analysed using analysis of variance followed by the Bonferroni multiple comparison test. A probability value of approximately 0.05 was adopted as the criterion for significance, although actual p-values are indicated when >0.0001.

5. Conclusion

Prenatal inhibition of the kynurenine pathway alters the expression of several proteins key to early brain development, accompanied by changes of neuronal activity and synaptic transmission. Of the eight proteins whose expression is altered n P21 neonates, the majority are components of receptors, while PSD-95 forms part of the postsynaptic receptor NMDAR complex with associated proteins and plays a role in the membrane

stabilization and functional sensitivity of the NMDA receptor (Kornau et al., 1995; Rutter and Stephenson, 2000). RhoB proteins are elements of transduction pathways that regulate NMDAR function. Three of the proteins affected – doublecortin, PCNA and sonic hedgehog - are concerned with neuron formation and maturation. The results therefore indicate that activity in the endogenous oxidative metabolism of tryptophan along the kynurenine pathway is likely to play a fundamental role in the early development of the brain, probably by affecting the expression of NMDAR subunits and proteins that modulate NMDAR function.

Acknowledgements

We thank Epsom Medical Research, the Peacock Trust and the Haddon Family Foundation Trust for supporting this work. OSK was funded by a postgraduate scholarship in Integrative Biology (BBSRC) and MP was supported by the Malaysian Government

REFERENCES

Afadlal, S., Polaboon, N., Surakul, P., Govitrapong, P., Jutapakdeegul, N., 2010. Prenatal stress alters presynaptic marker proteins in the hippocampus of rat pups. Neurosci. Lett., 470, 24-27.

Ahnert-Hilger, G., Holtje, M., Grosse, G., Pickert, G., Mucke, C., Nixdorf-Bergweiler, B., Boquet, P., Hofmann, F., Just, I., 2004. Differential effects of Rho GTPases on axonal and dendritic development in hippocampal neurons. J. Neurochem., 90, 9 – 18.

Alvarez, V.A., Ridenour, D.A., Sabatini, BL., 2007. Distinct structural and ionotropic roles of NMDA receptors in controlling spine and synapse stability. J. Neurosci., 27, 7365-7376

Angot, E., Loulier, K., Nguyen-Ba-Charvet, K.T., Gadeau, A.-P., Ruat, M., Traiffort, E. , 2008. Chemoattractive activity of Sonic Hedgehog in the adult subventricular zone modulates the number of neural precursors reaching the olfactory bulb. Stem Cells, 26, 2311-2320.

Aoto, J., Ting, P., Maghsoodi, B., Xu, N., Henkemeyer, M., Chen, K., 2007. Postsynaptic EphrinB3 promotes shaft glutamatergic synapse formation. J. Neurosci., 27, 7508-7519.

Baran, H., Schwarcz, R., 1990. Presence of 3-hydroxyanthranilic acid in rat-tissues and evidence for its production from anthranilic acid in the brain. J. Neurochem., 55, 738-744.

Behar, T.N., Scott, C.A., Greene, C.L., Wen, X.L., Smith, S.V., Maric, D., Liu, Q.Y., Colton, C.A, Barker, J.L **.**, 1999. Glutamate acting at NMDA receptors stimulates embryonic cortical neuronal migration. J. Neurosci., 19, 4449-4461.

Boegman, R.J., Eldefrawy, S.R., Jhamandas, K., Beninger, R.J., Ludwin, S.K., 1985. Quinolinic acid neurotoxicity in the nucleus basalis antagonized by kynurenic acid. Neurobiol. Aging, 6, 331-336.

Bourgin, C., Murai, K.K., Richter, M.& Pasquale, E.B., 2007. The EphA4 receptor regulates dendritic spine remodeling by affecting beta 1-integrin signaling pathways. J. Cell Biol., 178, 1295-1307

Brigman, J.L., Wright, T., Talani, G., Prasad-Mulcare, S., Jinde, S., Seabold, G.K., Mathur, P., Davis, M.I., Bock, R., Gustin, R.M., Colbran, R.J., Alvarez, V.A., Nakazawa, K., Delpire, E., Lovinger, D.M., Holmes, A., 2010. Loss of GluN2B-containing NMDA receptors in CA1 hippocampus and cortex impairs long-term depression, reduces dendritic spine density, and disrupts learning. J. Neurosci., 30, 4590-4600.

Carpenedo, R., Meli, E., Peruginelli, F., Pellegrini-Giampietro, D.E., Moroni, F., 2001. Kynurenine 3-mono-oxygenase inhibitors attenuate post-ischemic neuronal death in organotypic hippocampal slice cultures. J. Neurochem., 82, 1465-1471.

Chen, Y., Guillemin, G.J., 2009. Kynurenine metabolism in humans: disease and healthy states. Intern. J. Tryptophan. Res., 2, 1-19.

Chiarugi, A., Cozzi, A., Ballerini, C., Massacesi, L., Moroni, F., 2001. Kynurenine 3-mono-oxygenase activity and neurotoxic kynurenine metabolites increase in the spinal cord of rats with experimental allergic encephalomyelitis. Neuroscience, 102, 687-695.

Chiarugi, A., Moroni, F., 1999. Quinolinic acid formation in immune-activated mice: studies with (m-nitrobenzoyl)-alanine (mNBA) and 3,4-dimethoxy-[-N-4-(-3-nitrophenyl)thiazol-2yl]-benzenesulfonamide (Ro 61-8048), two potent and selective inhibitors of kynurenine hydroxylase. Neuropharmacology. 38, 1225-1233.

Clark, C., Mackay, G.M., Smythe, G.A., Bustamante, S., Stone, T.W., Phillips, S.R., 2005. Prolonged survival of a murine model of cerebral malaria by kynurenine synthesis inhibition. Infection, Immunity 73, 5249-5251.

Colonnese, M.T., Zhao, J.P., Constantine-Paton, M., 2005. NMDA receptor currents suppress synapse formation on sproutin axons in vivo. J. Neurosci., 25, 1291-1303.

.

Cozzi, A., Carpenedo, R., Moroni, F., 1999. Kynurenine hydroxylase inhibitors reduce ischemic brain damage: Studies with (m-nitrobenzoyl)-alanine (mNBA) and 3,4-dimethoxy-[-N-4-(nitrophenyl)thiazol-2YL]-benzenesulfonamide (Ro61-8048) in models of focal or global brain ischaemia. J. Cereb. Blood Flow Metab., 19, 771-777.

Cuppini, R., Sartini, S., Ambrogini P, Falcieri, E., Maltarello, M.C., Gallo, G., 1999. Control of neuron outgrowth by NMDA receptors. J. Submicrosc. Cytol. Pathol., 31, 31-40.

Dikranian, K., Ishimaru MJ, Tenkova T, Labruyere, J., Qin, Y.Q., Ikonomidou, C., Olney, J.W., 2001. Apoptosis in the in vivo mammalian forebrain. Neurobiol. Dis., 8, 359-379.

du Bois, T.M., Huang, X.F., 2007). Early brain development disruption from NMDA receptor hypofunction: relevance to schizophrenia. Brain Res. Rev., 53, 260-270.

Fagiolini, M., Katagiri, H., Miyamoto, H., Mori, H., Grant, S.G.N., Mishina, M., Hensch, T.K., 2003. Separable features of visual cortical plasticity revealed by N-methyl-D-aspartate receptor 2A signaling. Proc. Nat. Acad. Sci. U.S.A., 100, 2854-2859.

Forrest, C.M., Addae, J.I., Murthy, S., Darlington, L.G., Morris, B.J., Stone, T.W., 2011. Molecular changes associated with hippocampal long-lasting depression induced by the serine protease subtilisin-A. Europ. J. Neurosci., 34, 1241-1253

Gregoire, L., Rassoulpour, A., Guidetti, P., Samadi, P., Bedard, P J., Izzo, Ea., Schwarcz, R., Di Paolo, T., 2008. Prolonged kynurenine 3-hydroxylase inhibition reduces development of levodopa-induced dyskinesias in parkinsonian monkeys. Behav. Brain Res., 186, 161-167.

Gurdon, J.B., Bourillot, P.Y., 2001. Morphogen gradient interpretation. Nature, 413, 797-803.

Halim, N.D., Weickert, C.S., McClintock, B.W., Hyde, T.M., Weinberger, D.R., Kleinman, J,E., Lipska, B.K., 2003. Presynaptic proteins in the prefrontal cortex of patients with schizophrenia and rats with abnormal prefrontal development. Molec. Psychiat., 8, 797-810.

Hardingham, G.E., Bading, H., 2010. Synaptic versus extrasynaptic NMDA receptor signalling: implications for neurodegenerative disorders. Nature Rev. Neurosci., 11, 682-696.

Harris, L.W., Sharp, T., Gartlon, J., Jones, D.N.C., Harrison, P.J., 2003. Long-term behavioural, molecular and morphological effects of neonatal NMDA receptor antagonism. Europ. J. Neurosci., 18, 1706-1710.

Henderson, J.T., Georgiou, J., Jia, Z.P., Robertson, J., Elowe, S., Roder, J.C., Pawson, T., 2001. The receptor tyrosine kinase EphB2 regulates NMDA-dependent synaptic function Neuron, 32, 1041-1056

Heng, J.E., Zurakowski, D., Vorwerk, C.K., Grosskreutz, C.L., Dreyer, E.B., 1999. Cation channel control of neurite morphology. Develop. Brain Res., 113, 67-73

Herve, C., Beyne, P., Jamault, H., Delacoux, E., 1996. Determination of tryptophan and its kynurenine pathway metabolites in human serum by high-performance liquid chromatography with simultaneous ultraviolet and fluorimetric detection. J. Chromatogr B., 675, 157-161.

Hilmas, C., Pereira, E.F.R., Alkondon, M., Rassoulpour, A., Schwarcz, R., Albuquerque, E.X. , 2001. The brain metabolite kynurenic acid inhibits alpha 7 nicotinic receptor activity and increases non-alpha 7 nicotinic receptor expression: physiopathological implications J. Neurosci., 21, 7463-7473.

Honig, A., Rieger, L., Kapp, M., Sutterlin, M., Dietl, J., Kammerer, U., 2004. Indoleamine 2,3-dioxygenase (IDO) expression in invasive extravillous trophoblast supports role of the enzyme for materno-fetal tolerance. J. Reprod. Immunol., 61, 79-86.

Hor, C.H.H., Tang, B.L., 2010). Sonic hedgehog as a chemoattractant for adult NPCs. Cell Adhesion and Migration, 4, 1-3.

Ikonomidou, C., Bosch, F., Miksa, M., Bittigau, P., Vockler, J., Dikranian, K., Tenkova, T.I., Stefovska, V., Turski, L., Olney, J.W., 1999. Blockade of NMDA receptors and apoptotic neurodegeneration in the developing brain. Science, 283, 70-74.

Iwasato, T., Datwani, A., Wolf, A.M., Nishiyama, H., Taguchi, Y., Tonegawa, S., Knopfel, T., Erzurumlu, R.S., Itohara, S., 2000. Cortex-restricted disruption of NMDAR1 impairs neuronal patterns in the barrel cortex. Nature, 406, 726-731.

Klein, R., 2004. Eph/ephrin signaling in morphogenesis, neural development and plasticity. Curr. Opin. Cell. Biol., 16,580-589.

Koh, C.-G., 2006. RhoGTPases and their regulators in neuronal function and development. Neurosignals, 15, 228-237.

Komuro, H., Rakic, P., 1993. Modulation of neuronal migration by NMDA receptors. Science, 260, 95-97.

Kornau, H.C., Schenker, L.T., Kennedy, M.B., Seeburg, P.H., 1995. Domain interaction between NMDA receptor subunits and the postsynaptic density protein PSD-95. Science, 269, 1737-1740.

Larson, J., Wong, D.L., Lynch, G., 1986. Patterned stimulation at the theta frequency is optimal for the induction of hippocampal long-term potentiation. Brain Res., 368, 347-350.

Li, Z., Aizenman, C.D., Cline, H.T., 2002. Regulation of RhoGTPases by crosstalk and neuronal activity in vivo. Neuron, 33, 741-750.

Ligam, P., Manuelpillai, U., Wallace, E.M., Walker, D., 2005. Localisation of indoleamine 2,3-dioxygenase and kynurenine hydroxylase in the human placenta and decidua: Implications for role of the kynurenine pathway in pregnancy. Placenta, 26, 498-504.

Luo, L.Q., 2000. RhoGTPases in neuronal morphogenesis. Nature Revs. Neurosci., 1, 173-180.

Martinez, A,, Soriano, E., 2005. Functions of ephrin/Eph interactions in the development of the nervous system: Emphasis on the hippocampal system. Brain Res. Revs., 49, 211-226.

Maycox, P. R., Kelly, F., Taylor, A., Bates, S., Reid, J., Logendra, R., Barnes, M. R., Larminie, C., Jones, N., Lennon, M., Davies,T.I., Hagan, J. J., Scorer, C.A., Angelinetta, C., Akbar, T., Hirsch, S., Mortimer, A. M., Barnes, T. R. E., de Belleroche, J., 2009. Analysis of gene expression in two large schizophrenia cohorts identifies multiple changes associated with nerve terminal function. Molec. Psychiat., 14, 1083-1094.

McKay, S. Griffiths, N.H., Butters, P.A., Thubron, E.B., Hardingham, G.E., Wyllie, D.J.A., 2012. Direct pharmacological monitoring of the developmental switch in NMDA receptor subunit composition using TCN 213, a GluN2A-selective, glycine-dependent antagonist. Brit. J. Pharmacol., 166, 924-937.

McNair, K., Spike. R., Guilding, C., Prendergast, G.C., Stone, T.W., Cobb, S.R., Morris, B.J., 2010. A role for RhoB in synaptic plasticity and the regulation of neuronal morphology. J. Neurosci., 30, 3508-3517.

Nadri, C., Agam, G., 2009. Perinatal oxygen restriction does not result in reduced rat frontal cortex: synaptophysin levels at adulthood as opposed to postmortem findings in schizophrenia. J. Molec. Neurosci., 37, 60-66.

Narumiya, S., Ishizaki, T., Watanabe, N., 1997. Rho effectors and reorganization of actin cytoskeleton. FEBS Lett., 410, 68-72.

Norenberg, W., Hofmann, F., Illes, P., Aktories, K., Meyer, DK., 1999. Rundown of somatodendritic N-methyl-D-aspartate (NMDA) receptor channels in rat hippocampal neurones: evidence for a role of the small GTPase RhoA. Brit. J. Pharmacol., 127, 1060-1063.

O'Kane, E.M., Stone, T.W., Morris, B.J., 2003a. Activation of Rho GTPases by synaptic transmission in the hippocampus. J. Neurochem., 87, 1309-1312

O'Kane, E.M., Stone, T.W., Morris, B.J., 2003b. Distribution of Rho family GTPases in the adult rat hippocampus and cerebellum. Molec Brain Res., 114: 1-8

Palma, V., Lim, D.A., Dahmane, N., Sanchez, P., Brlonne, T.C., Herzberg, C.D., Gitton, Y., Carleton, A., Alvarez-Buylla, A., Altaba, A.R.I., 2005. Sonic hedgehog controls stem cell behavior in the postnatal and adult brain. Development, 132, 335-344.

Perkins, M.N., Stone, T.W., 1982. An iontophoretic investigation of the action of convulsant kynurenines and their interaction with the endogenous excitant quinolinic acid. Brain Res., 247, 184-187

Poulaki, V., Benekou, A, Bozas E, Bolaris, S., Stylianopoulou, F., 1999. P53 expression and regulation by NMDA receptors in the developing rat brain. J. Neurosci. Res., 56, 427-440.

Rajan I,, Cline, H.T., 1998. Glutamate receptor activity is required for normal development of tectal cells dendrites in vivo. J. Neurosci., 18, 7836-7846.

Rammes, G. Starker, L.K., Haseneder, R., Berkmann, J., Plack, A., Zieglgansberger, W., Ohl, F., Kochs, E.F., Blobner, M., 2009. Isoflurane anaesthesia reversibly improves cognitive function and long-term potentiation (LTP) via an up-regulation in NMDA receptor 2B subunit expression. Neuropharmacology, 56, 626-636.

Rodgers, J., Stone, T.W., Barratt, M.P., Bradley, B., Kennedy, P.G., 2009. Kynurenine pathway inhibition reduces central nervous system inflammation in a model of human African trypanosomiasis. Brain 132, 1259-1267.

Rosenmund, C., Stevens, C.F., 1996. Definition of the readily releasable pool of vesicles at hippocampal synapses. Neuron, 16, 1197-1207.

Rover, S., Cesura, A.M., Huguenin, P., Kettler, R., Szente, A., 1997. Synthesis and biochemical evaluation of N-(4-phenylthiazol-2-yl)benzenesulfonamides as high-affinity inhibitors of kynurenine 3-hydroxylase. J. Med. Chem., 40, 4378-4385.

Rutter, A.R., Stephenson, F.A., 2000. Coexpression of postsynaptic density-95 protein with NMDA receptors results in enhanced receptor expression together with a decreased sensitivity to L-glutamate. J. Neurochem., 75, 2501-2510.

Saviane, C., Savtchenko, L.P., Raffaelli, G., Voronin, L.L, Cherubini. E., 2002. Frequency-dependent shift from paired-pulse facilitation to paired-pulse depression at unitary CA3-CA3 synapses in the rat hippocampus. J. Physiol.(Lond.), 544, 469-476.

Scharfman, H.E., Hodgkins, P.S., Lee, S.C., Schwarcz, R., 1999. Quantitative differences in the effects of de novo produced and exogenous kynurenic acid in rat brain slices. Neurosci. Lett., 274, 111-114.

Segura, I., Essmann, C.L.,Weinges, S., Acker-Palmer, A.(2007. Grb4 and GIT1 transduce ephrinB reverse signals modulating spine morphogenesis and synapse formation. Nature Neurosci., 10, 301-310.

Shibata, K., 1988. Fluorimetric micro-determination of kynurenic acid, an endogenous blocker of neurotoxicity, by high-performance liquid-chromatography. 430, 376-380.

Sims, J.R., Lee, S.W., Topalkara, K., Qiu, J., Xu, J.,Zhou, Z., Moskowitz, M.A., 2009. Sonic hedgehog regulates ischemia/hypoxia-induced neural progenitor proliferation. Stroke, 40, 3618-3626.

Stone, T.W., 1993. The neuropharmacology of quinolinic and kynurenic acids. Pharmacol. Revs., 45, 309-379.

Stone, T.W., 2001. Kynurenines in the CNS - from obscurity to therapeutic importance. Progr. Neurobiol., 64, 185-218

Stone, T.W., 2007. Kynurenic acid blocks nicotinic synaptic transmission to hippocampal interneurons in young rats. Europ. J. Neurosci., 25, 2656 – 2665

Stone, T.W., Darlington, L.G., 2002. Endogenous kynurenines as targets for drug discovery and development. Nature Revs. Drug Disc., 1, 609-620.

Stone, T.W., Perkins, M.N., 1981. Quinolinic acid: a potent endogenous excitant at amino acid receptors in CNS. Europ. J. Pharmacol., 72, 411-412.

Takasu, M.A., Dalva, M.B., Zigmond, R.E., Greenberg, M.E., 2002. Modulation of NMDA receptor-dependent calcium influx and gene expression through EphB receptors. Science, 295, 491-494.

Traiffort, E., Moya, K.L., Faure, H., Hassig, R., Ruat, M., 2001. High expression and anterograde axonal transport of aminoterminal sonic hedgehog in the adult hamster brain. Europ. J. Neurosci., 14, 839-850.

Traiffort, E., Angot, E., Ruat, M., 2010. Sonic hedgehog in the mammalian brain. J. Neurochem., 113, 576-590.

Ueda, T., Otsuka, H., Goda, K., Ishiguro, I., Naito, J., Kotake, Y., 1978. Metabolism of [carboxyl-C-14]-anthranilic acid .1. incorporation of radioactivity into NAD+ and NADP+. J. Biochem. 84, 687-696

Ultanir, S.K., Kim, J.E., Hall, B.J., Deerinck, T., Ellisman, M., Ghosh, A., 2007. Regulation of spine morphology and spine density by NMDA receptor signaling in vivo. Proc. Nat. Acad. Sci. U.S.A., 104, 19553-19558.

Urenjak, J., Obrenovitch, T.P., 2000). Kynurenine 3-hydroxylase inhibition in rats: Effects on extracellular kynurenic acid concentration and N-methyl-D-aspartate-induced depolarisation in the striatum. J. Neurochem., 75, 2427-2433.

Van Aelst, L., Cline, H.T., 2004. RhoGTPases and activity-dependent dendrite development. Curr. Opin. Neurobiol., 14, 297-304.

Von Bohlen und Halbach, O., 2011. Immunohistological markers for proliferative events, gliogenesis and neurogenesis within the adult hippocampus. Cell Tiss. Res., 2011, 345,1-19.

Waldeck, R.F., Pereda, A., Faber, D.S., 2000. Properties and plasticity of paired-pulse depression at a central synapse. J. Neurosci., 20, 5312-5320.

Wang, L.Y., Kaczmarek, L.K., 1998. High-frequency firing helps replenish the readily releasable pool of synaptic vesicles. Nature, 394, 384-388.

Zucker, R.S., 1989. Short-term synaptic plasticity. Ann. Rev. Neurosci. 12, 13-31.

Zwilling, D., Huang, S.Y., Sathyasaikumar, K.V., Notarangelo, F.M., Guidetti, P., Wu, H.Q., Lee, J., Truong, J., Andrews-Zwilling, Y., Hsieh, E.W., Louie, J.Y., Wu, T., Scearce-Levie, K., Patrick, C., Adame, A., Giorgini, F., Moussaoui, S., Laue, G., Rassoulpour, A., Flik, G., Huang, Y., Muchowski, J.M., Masliah, E., Schwarcz, R., Muchowski, P.J., 2011. Kynurenine 3-Monooxygenase inhibition in blood ameliorates Neurodegeneration. Cell, 145, 863-874.

Figure legends

Figure 1. HPLC analysis of tryptophan metabolites after the administration of Ro61-8048.

A. Major components of the kynurenine pathway. The enzyme kynurenine-3-monoxygenase (KMO) converts kynurenine into 3-hydroxykynurenine. Inhibition of this enzyme by Ro61-8048 forces the transamination of kynurenine to kynurenic acid via kynurenine aminotransferase.

B. Bar charts showing the kynurenine pathway metabolite levels detected by High Performance Liquid Chromatography (HPLC) 5h following a single maternal injection of Ro61-8048 (R) or saline vehicle (S) on embryonic day 18 (E18). Panels summarise (a) the maternal plasma levels (μM) or brain concentrations in the mother (b,c) and embryos (d,e) (per gramme wet weight; g.w.w.) of kynurenine and kynurenic acid 5h (b,d) and 24h (c,e) after the administration of Ro61-8048. Bars indicate mean ± s.e.mean for maternal plasma and brain samples (n=3) from 3 separate litters, or embryo brain samples (n=6) where 2 embryo brains/litter were analysed from each of the 3 litters.

* P < 0.05; ** P < 0.01; ***P < 0.001 unpaired *t* test.

Figure 2. Protein expression in the brain of embryos after prenatal Ro61-8048.

Bar charts showing the quantified expression of (**A**) GluN2A (180kDa) and GluN2B (180kDa) proteins in the brains of embryos 5h after the prenatal administration of Ro61-8048, while **(B)** shows the expression of sonic hedgehog (SHH, 45kDa) and NFkB (65kDa) at 24h post-administration. The bars indicate the mean ± s.e.mean (n = 6) in arbitrary units of optical density (OD) expressed as the ratio of test protein to actin. Representative western blots above each chart illustrate the data obtained from animals exposed to the

saline vehicle (S) or Ro61-8048 (R) and show the relevant protein and the corresponding actin (42kDa) blot used as a housekeeping marker. * P < 0.05; ** P < 0.01 unpaired *t* test.

Figure 3. Hippocampal function in P21 offspring after prenatal Ro61-8048.

The graphs show the increase in size of (**A**) field excitatory postsynaptic potentials (fEPSPs) and (**B**) population spikes in the hippocampal CA1 region as a function of stimulus current, which was increased from threshold in steps of 5μA (A) or 10μA (B). The inset of panel (A) illustrates sample fEPSPs for a typical slice. Ordinate values are expressed in (A) relative to the maximum fEPSP obtained before any appearance of a population spike, and in (B) relative to the maximum population spike amplitude obtainable. The symbols indicate mean ± s.e.mean (n = 16 controls and 15 treated) for animals exposed to saline vehicle (solid circles) or Ro61-8048 (open circles).

Paired-pulse data are shown for the ratio of fEPSPs recorded in stratum radiatum produced by each of the two paired stimuli (**C**), and the ratio of population spikes recorded in stratum pyramidale (**D**). The change in population spike ratio at different rates of paired-pulse presentation from 0.05 to 1Hz is shown in (E) The symbols indicate mean ± s.e.mean (n = 10 controls and 12 treated) for animals exposed to saline vehicle (solid circles) or Ro61-8048 (open circles).

* P < 0.05; ** P < 0.01; ***P < 0.001 using the Bonferroni test for multiple comparisons following ANOVA (P < 0.0001, see text). Number of samples is indicated above.

Figure 4. Adult hippocampal plasticity after prenatal exposure to Ro61-8048.

Panel (**A**) illustrates long-term potentiation in the two groups of offspring following theta-burst stimulation at the arrow. The inset records illustrate a control fEPSP immediately before stimulation and the potentiated response 40min later in a slice from a control animal (**B**) or an animal exposed *in utero* to Ro61-8048 (**C**).

The symbols indicate mean ± s.e.mean (n = 6). Calibrations 0.5mV and 10ms.

*** P < 0.001 for the final 5 minutes of recording (ANOVA).

Panel **(D**) illustrates long-term depression in the two groups of offspring induced by two periods of low frequency stimulation indicated by the bars on the abscissa at stim1 and stim2 (see text). The inset records illustrate a control fEPSP immediately before stim1 and the depressed responses 20min after stim1 and 20 min after stim2 in a slice from a control animal (**E**) or an animal exposed in utero to Ro61-8048 (**F**).

The symbols indicate mean ± s.e.mean (n = 6). There were no significant differences between the control and treated slices.

Calibrations 1mV, 10ms for the control records and 0.5mV, 10ms for drug-exposed slices.

Figure 5. Protein expression in the brains of P21 offspring after prenatal Ro61-8048.

Bar charts showing the quantified expression of GluN1 (130kDa), GluN2A (180kDa), GluN2B (180kDa), PSD-95 (95kDa), RhoA (24kDa) and RhoB (25kDa) proteins in the brains of P21 offspring following their prenatal exposure to Ro61-8048. The bars indicate the mean ± s.e.mean (n = 6) in arbitrary units of optical density (OD) expressed as the ratio of test protein to actin. Representative western blots above each chart illustrate the data obtained from animals exposed to the saline vehicle (S) or Ro61-8048 (R) and show the relevant protein and the corresponding actin (42kDa) blot used as a housekeeping marker. * P < 0.05; ** P < 0.01 unpaired *t* test.

Figure 6. Protein expression in the brains of P21 offspring after prenatal Ro61-8048.

Bar charts showing the quantified expression of PCNA (36kDa), doublecortin (40kDa), sonic hedgehog (SHH, 45kDa), tyrosine hydroxylase (TH, 60kDa), α-synuclein (19kDa) and DISC1 (100kDa) proteins in the brains of P21 offspring following their prenatal exposure to Ro61-8048. The bars indicate the mean $\pm$ s.e.mean (n = 6) in arbitrary units of optical density (OD) expressed as the ratio of test protein to actin. Representative western blots above each chart illustrate the data obtained from animals exposed to the saline vehicle (S) or Ro61-8048 (R) and show the relevant protein and the corresponding actin (42kDa) blot used as a housekeeping marker.

* $P < 0.05$ unpaired *t* test.

Figure 1

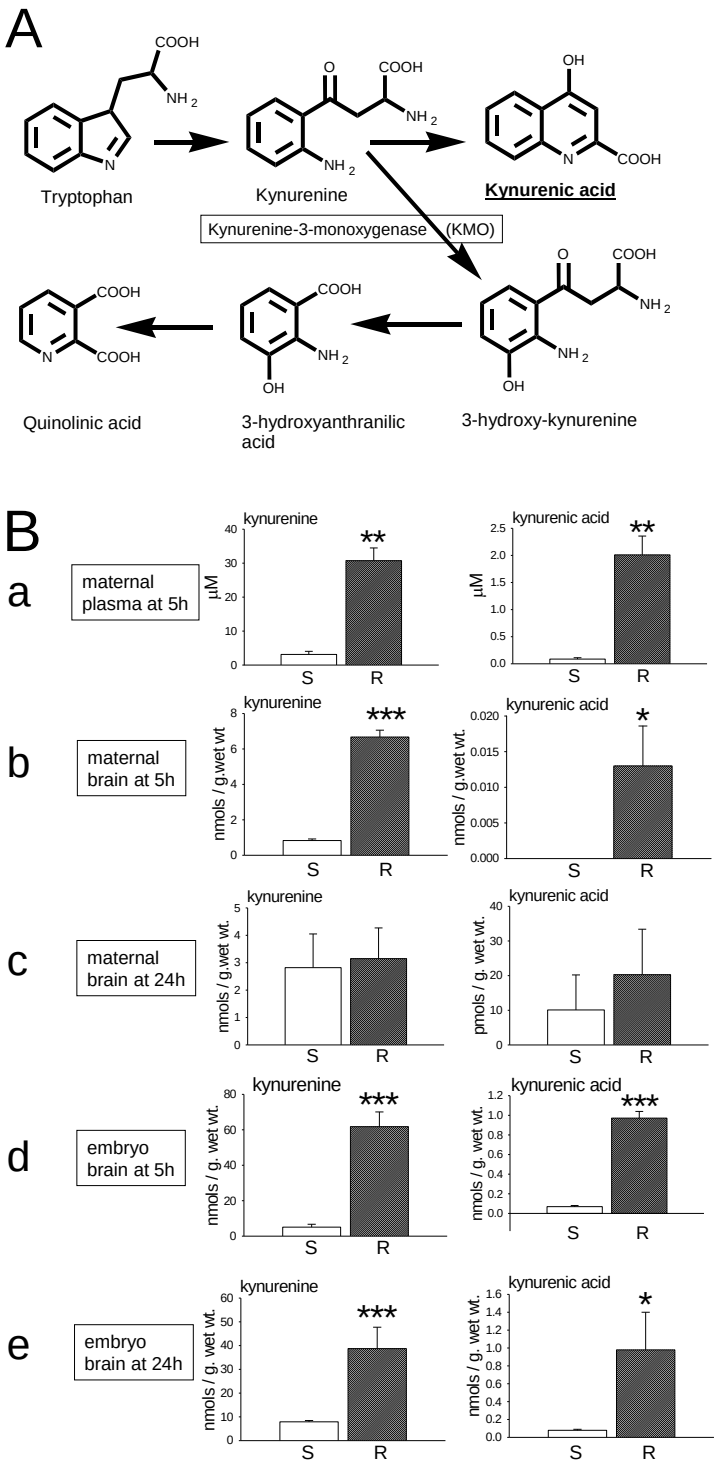
A
Tryptophan
Kynurenine
Kynurenic acid
Kynurenine-3-monoxygenase (KMO)
Quinolinic acid
3-hydroxyanthranilic acid
3-hydroxy-kynurenine
B
a
maternal plasma at 5h
b
maternal brain at 5h
c
maternal brain at 24h
d
embryo brain at 5h
e
embryo brain at 24h
kynurenine
kynurenic acid
µM
nmols / g.wet wt
nmols / g. wet wt.
pmols / g. wet wt.
S
R

Figure 2

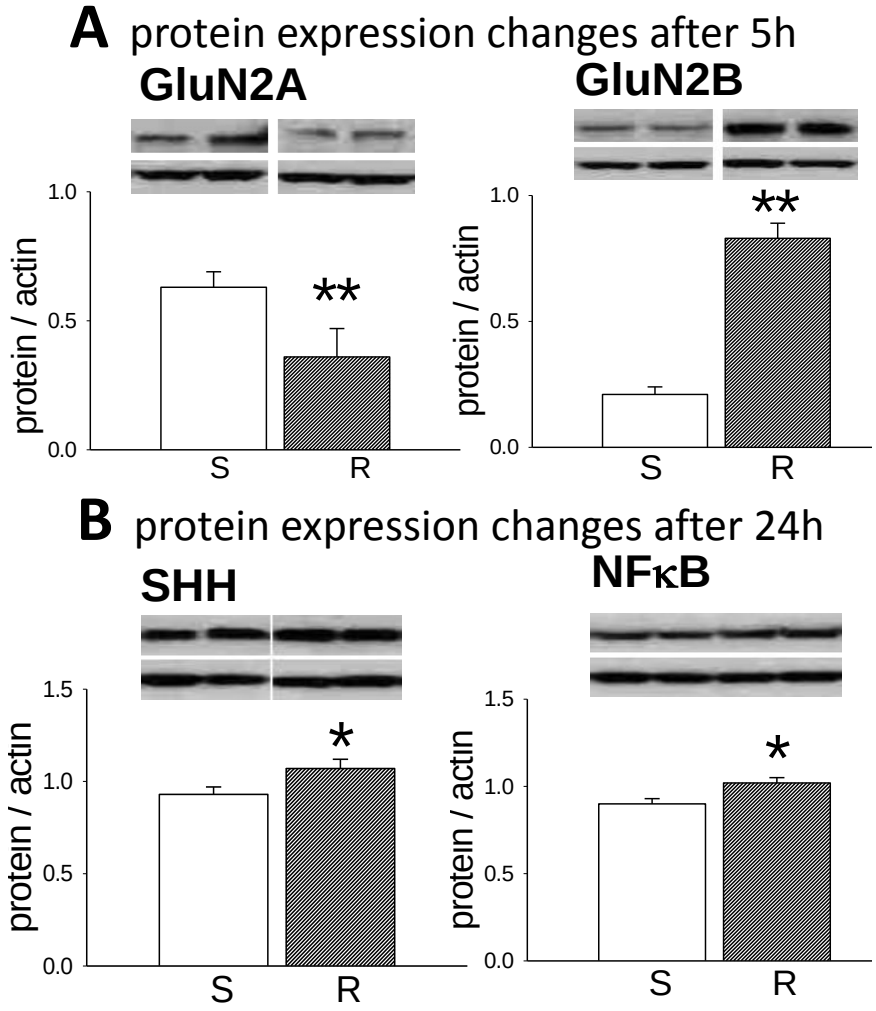
A protein expression changes after 5h
GluN2A
GluN2B
protein / actin
1.0
0.5
0.0
**
**
S
R
B protein expression changes after 24h
SHH
NFκB
protein / actin
1.5
1.0
0.5
0.0
*
*
S
R

Figure 3

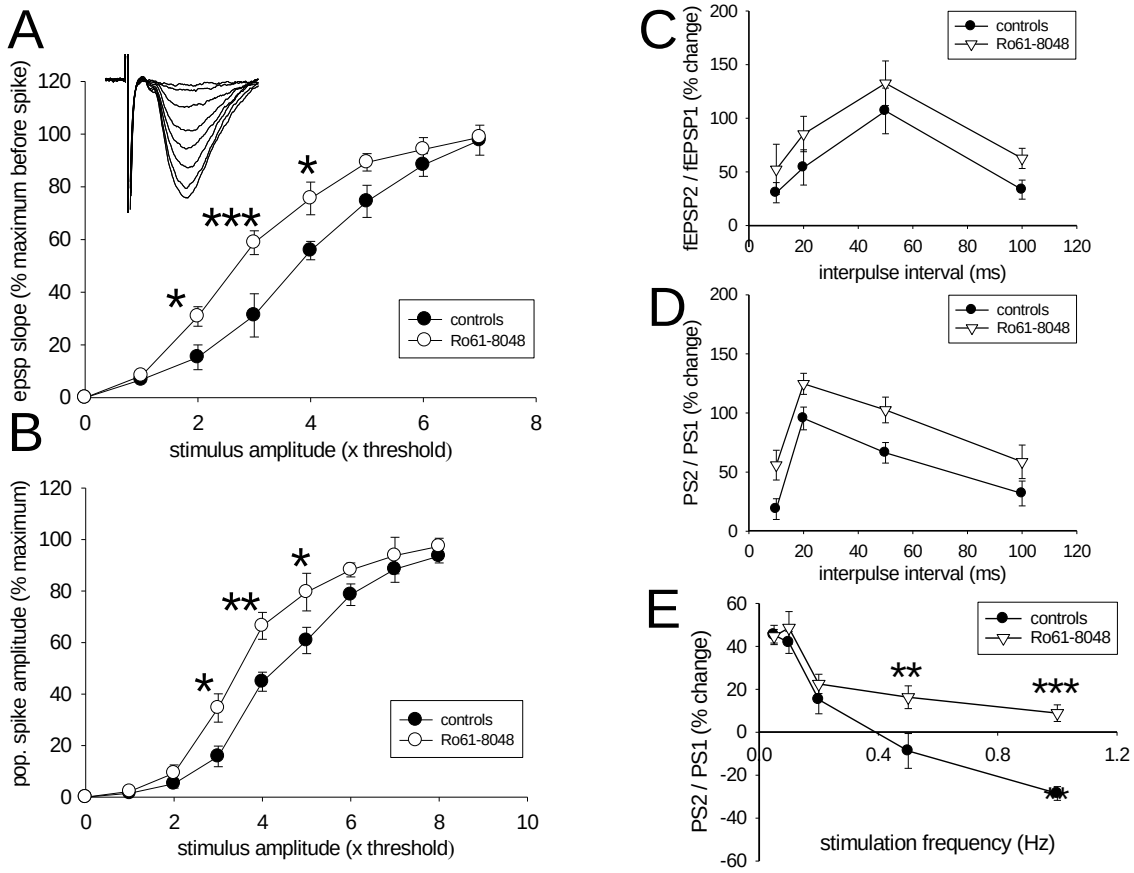
A
epsp slope (% maximum before spike)
stimulus amplitude (x threshold)
controls
Ro61-8048
B
pop. spike amplitude (% maximum)
stimulus amplitude (x threshold)
controls
Ro61-8048
C
fEPSP2 / fEPSP1 (% change)
interpulse interval (ms)
controls
Ro61-8048
D
PS2 / PS1 (% change)
interpulse interval (ms)
controls
Ro61-8048
E
PS2 / PS1 (% change)
stimulation frequency (Hz)
controls
Ro61-8048

Figure 4

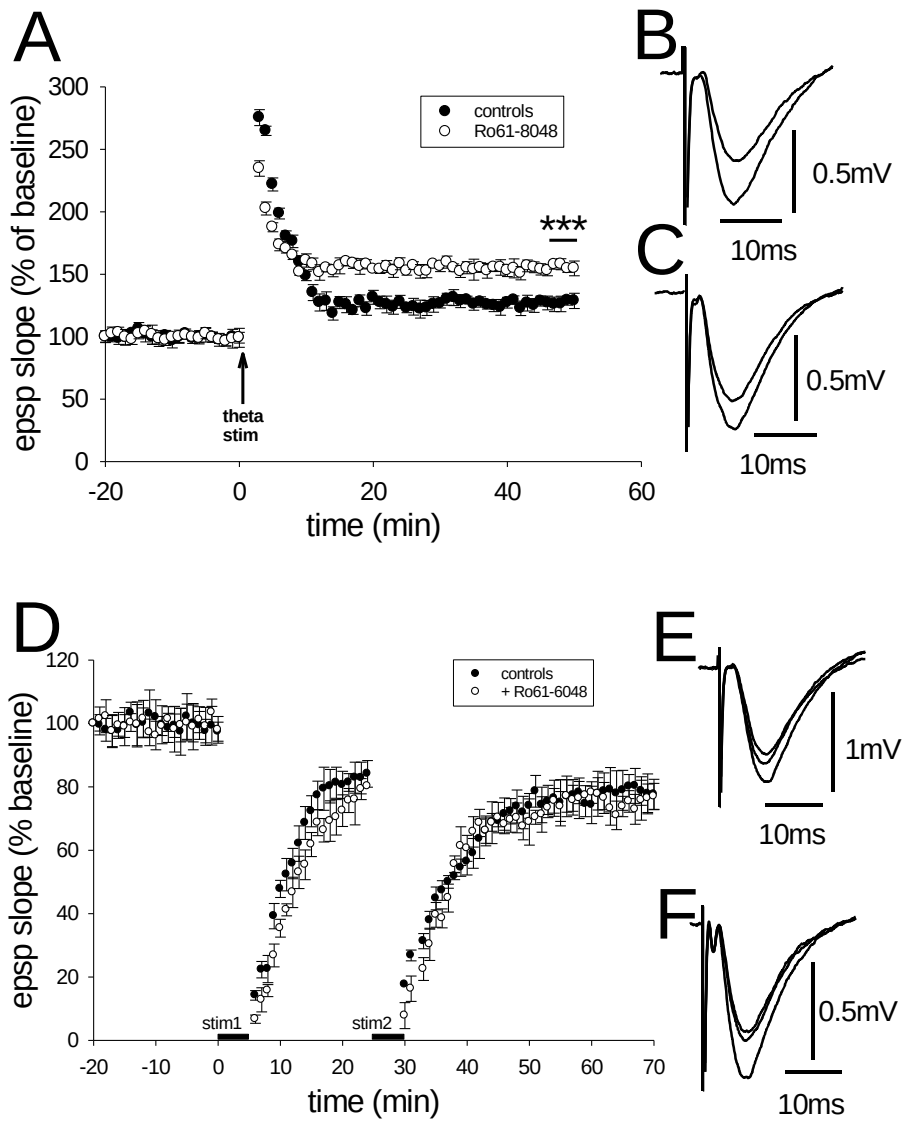
A
B
C
D
E
F
epsp slope (% of baseline)
time (min)
controls
Ro61-8048
***
theta stim
0.5mV
10ms
0.5mV
10ms
controls
+ Ro61-6048
stim1
stim2
1mV
10ms
0.5mV
10ms

Figure 5

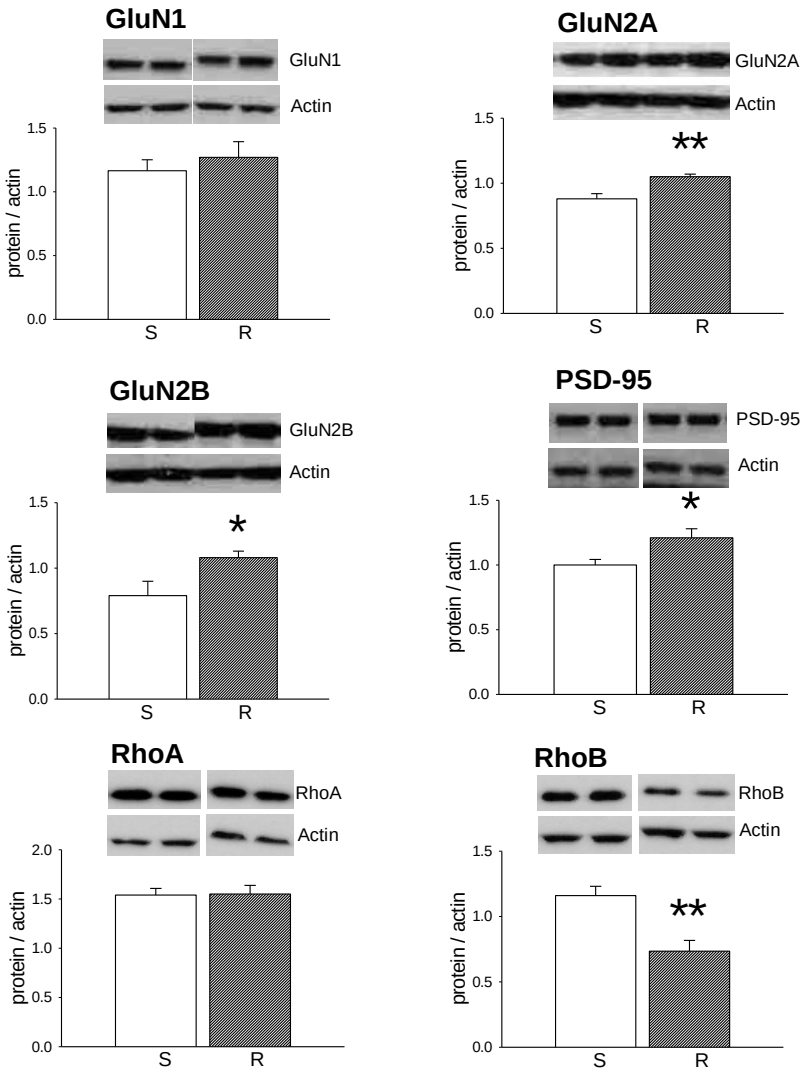
GluN1
GluN1
Actin
protein / actin
1.5
1.0
0.5
0.0
S
R
GluN2A
GluN2A
Actin
**
protein / actin
1.5
1.0
0.5
0.0
S
R
GluN2B
GluN2B
Actin
*
protein / actin
1.5
1.0
0.5
0.0
S
R
PSD-95
PSD-95
Actin
*
protein / actin
1.5
1.0
0.5
0.0
S
R
RhoA
RhoA
Actin
protein / actin
2.0
1.5
1.0
0.5
0.0
S
R
RhoB
RhoB
Actin
**
protein / actin
1.5
1.0
0.5
0.0
S
R

Figure 6

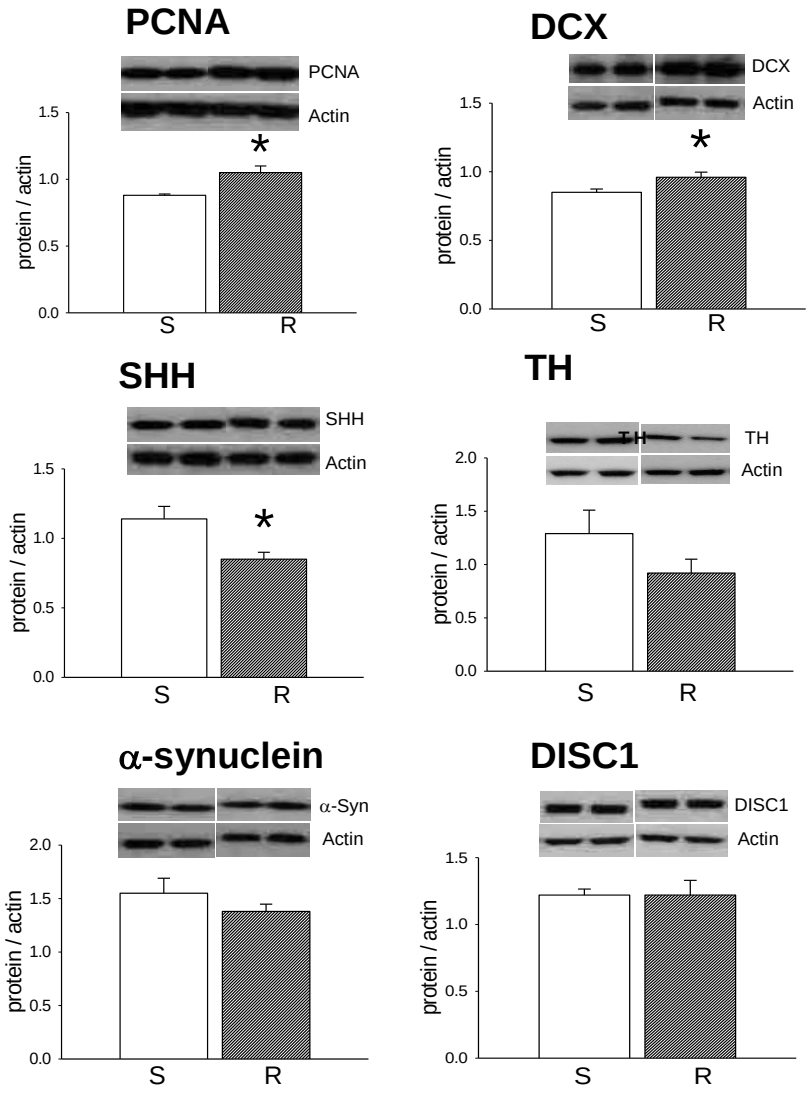
PCNA
PCNA
Actin
protein / actin
1.5
1.0
0.5
0.0
*
S
R
DCX
DCX
Actin
protein / actin
1.5
1.0
0.5
0.0
*
S
R
SHH
SHH
Actin
protein / actin
1.5
1.0
0.5
0.0
*
S
R
TH
TH
Actin
protein / actin
2.0
1.5
1.0
0.5
0.0
S
R
α-synuclein
α-Syn
Actin
protein / actin
2.0
1.5
1.0
0.5
0.0
S
R
DISC1
DISC1
Actin
protein / actin
1.5
1.0
0.5
0.0
S
R